Z. Phys. C 58, 95–108 (1993)

ZEITSCHRIFT
FÜR PHYSIK C

Influence of the internal degrees of freedom on J/ψ suppression*

J. Cugnon, P.-B. Gossiaux**

Université de Liège, Institut de Physique au Sart Tilman, Bâtiment B.5, B-4000 Liège 1, Belgium

Received 2 October 1992

Abstract. The influence of the internal degrees of freedom on the J/ψ suppression in relativistic heavy ion collisions is studied in the frame of a quantum-mechanical model. The wave function for the internal motion of a $c-\bar{c}$ pair obeys a time-dependent Schrödinger equation with a potential reflecting the properties of the medium in which the pair is travelling. The initial wave function is evaluated theoretically. An imaginary potential is introduced to account for the loss of probability due to the coupling to the $D-\bar{D}$ channels. The J/ψ survival probability is estimated as a function of the time spent inside the plasma. The connection with semi-classical approximations based on the formation time concept is established. The quantum-mechanical effects are exhibited and shown to lead to a smooth perpendicular momentum dependence of the J/ψ suppression, in agreement with the recent reanalysis of the NA38 data by Gupta and Satz. Several plasma scenarios, including or not the presence of a mixed phase are investigated and the effect of the quantum-mechanical treatment is analyzed for each of them. It is shown that the data do not constraint the plasma scenario very strongly, but indicate the possibility of having a mixed phase with a rather long lifetime.

1 Introduction

A great deal of interest has been devoted in the last years to the J/ψ propagation in various media. It was triggered by the suggestion, done by Matsui and Satz [1], that the J/ψ suppression could provide a signature of the quark-gluon plasma. However, most of the models for the propagation of a J/ψ rely on the cross-section picture and/or on the multiple scattering formalism. They do not pay attention to the internal structure of the J/ψ, implicitly assuming that the $c-\bar{c}$ pair is formed immediately in the J/ψ state and remains in this state, except if the J/ψ disappears. However, it is expected that the $c-\bar{c}$ pair is formed in a state which is not the J/ψ state and it is often considered [2, 3] that it resembles the J/ψ at later times only (this idea is often referred to under the label of "formation time"). Furthermore this state may evolve, owing to the interaction with the medium.

In this paper, we study a model which handles the effect of the internal structure of the $c-\bar{c}$ pair in a simple framework. Basically, we assume that the internal degrees of freedom of the $c-\bar{c}$ pair can be described by a time-dependent Schrödinger equation, using a real potential which reflects the influence of the medium and an imaginary part which describes the coupling to the absorption channels. This model, without imaginary part, has already been proposed in [4, 5], for the propagation in the plasma only. Here, we, in addition, will study the evolution through a mixed phase, for which semi-classical concepts (like formation time) have little intuitive meaning. Adopting a simple scenario for the plasma evolution, we will compare our results with those of semi-classical approaches, which neglect internal structure and are based on the formation time concept.

The paper is organized as follows. In Sect. 2, we describe our model for the propagation of a $c-\bar{c}$ pair and display its main properties. In Sect. 3, we discuss the question of the initial state and the possible information on this state which can be extracted from both experiment and theory. Section 4 presents our basic results for the evolution of the $c-\bar{c}$ wave packet as function of time. In Sect. 5, we show the J/ψ content for various plasma scenarios, including a mixed phase. We try to disentangle the influence of the plasma lifetime, of the duration of plasma-hadron phase transition and of the finite size of the system. We also compare with the semi-classical results in the same scenarios, exhibiting in this way the importance of the quantum-mechanical treatment. A tentative comparison with the experimental data of NA38 collaboration is presented in Sect. 6 and the implications on the plasma are briefly discussed. Section 7 is devoted

* Work supported by contract SPPS-IT/SC/29
** Research Assistant, National Fund for Scientific Research (Belgium)

to a discussion of the physics of the model, of its validity and of its potentialities.

2 The model

Let us consider a $c-\bar{c}$ pair rapidly travelling in some environment and let us concentrate on the internal motion of the pair. We assume that the latter can be described, as for the static properties of the charmonium, by Schrödinger quantum mechanics. The time evolution of the relative motion wave function $\psi(\mathbf{r}, t)$ can then be described by the time-dependent Schrödinger equation

$$i\hbar \frac{\partial \psi}{\partial t}(\mathbf{r}, t) = \left\{ -\frac{\hbar^2 \Delta}{m_c} + V(\mathbf{r}, t) - i W(\mathbf{r}) \right\} \psi(\mathbf{r}, t), \tag{2.1}$$

where m_c is the mass of the charmed quark. The basic premise of the model is the assumption that the influence of the medium on the $c-\bar{c}$ pair at time t can be embodied by a potential $V(\mathbf{r}, t)$, changing with time when the conditions of the environment are changing. This assumption implies that the translational motion of the pair is decoupled from its internal motion, which seems reasonable for a rapidly moving pair in a homogeneous medium. The same assumption has been proposed in [4, 5], where a similar model is studied for propagation in a plasma only.

In the present model, we introduce an imaginary part $W(r)$, which aims at describing the loss of probability from the pure $c-\bar{c}$ channel, due to the coupling to $D-\bar{D}$ channels [6, 7]. As explained in our previous work [6], the introduction of an imaginary potential of the type

$$W = W_0 \theta(r-L), \tag{2.2}$$

where θ is the Heaviside function, in the static charmonium hamiltonian is able to reproduce the hadronic widths of the charmonium (and bottonium) states above the $D-\bar{D}(B-\bar{B})$ channels. The r-dependence of the imaginary part is in keeping with the picture of string breaking: the string linking the c and $\bar{c}$ quarks has to be stretched sufficiently to be broken. We here assume for simplicity that the imaginary potential can be taken as time-independent. The values of the parameters W_0 and L are given in [6].

Let us consider a $c-\bar{c}$ pair created in a relativistic heavy ion collision. We assume that this pair is produced in a nucleon-nucleon collision at the very beginning of the process, like in free space. As in [2, 3], we assume that the pair is created in the supposedly formed plasma. The $c-\bar{c}$ pair under study will spent some time in the plasma, and then later on in a mixed phase and finally in an environment where it can be considered as in free space (see Sect. 5 for details). Therefore, we adopt the following time-dependent potential

$$V(\mathbf{r}, t) = -K_1 \frac{f(r)}{r} e^{-r/r_D}, \quad 0 < t < \tau_p \tag{2.3a}$$

$$-K_1 \frac{f(r)}{r} \exp\left[-r/r_D \left(1 - \frac{t-\tau_p}{\tau_m} \right) \right]$$

$$+Kr \frac{t-\tau_p}{\tau_m}, \quad \tau_p < t < \tau_p + \tau_m. \tag{2.3b}$$

Between τ_p and $\tau_p+\tau_m$, the potential interpolates smoothly between the Debye screened potential (2.3a) prevailing inside the plasma and the usual charmonium potential, which is totally restored at time $\tau_f = \tau_p + \tau_m$. The parameters K_1 and K and the function $f(r)$ are given in [8], while r_D is chosen as $r_D = 0.3$ fm, after [9].

We are interested in the components of the wave packet $\psi(\mathbf{r}, t)$ along the eigenstates of the static (real) charmonium hamiltonian ψ_i:

$$P_i(t) = |\langle \psi_i | \psi(\mathbf{r}, t) \rangle|^2, \tag{2.4}$$

where $i = J/\psi, \psi', \psi'', \ldots$ The potential (2.3) being central, there is no mixing between states of different angular momenta. Without the potential $W(\mathbf{r})$, the quantities $P_i(t)$ would remain constant for $t > \tau_f$. In the presence of $W(\mathbf{r})$, they then decay regularly, *except* $P_{J/\psi}$ and $P_{\psi'}$, which stay constant, owing to the fact that the absorption region $(r > L)$ lies beyond the radial extension of the corresponding components [6].

3 The initial state

We will assume that the $c-\bar{c}$ pair is formed as in free space proton-proton collisions. Therefore, in the Schrödinger picture, the content of the initial $c-\bar{c}$ wave packet in J/ψ (and ψ') should be given (in intensity) by the relative $p-p$ cross-sections. We here quickly review what is known both experimentally and theoretically about the initial wave packet.

3.1 Experimental indications

We focus our attention on the data at $\sqrt{s} = 20$ GeV, which is the nucleon-nucleon c.m. energy in the SPS heavy ion experiments. What is basically known is the following: (i) the total open charm production σ_{oc} is equal to $\left(39^{+25}_{-19}\right)$ μb [10]; (ii) the inclusive J/ψ production is equal to (52.95 ± 20.0) nb [11]. Although it is conceivable that open charm production may not simply proceed by the creation of a pure $c-\bar{c}$ pair, these data suggest that the $c-\bar{c}$ initial packet has a very small J/ψ content (a few percent at the most). This corresponds either to a spherical $c-\bar{c}$ wave packet with a very small overlap with the J/ψ wave function or to a non spherical wave packet with a small $\ell = 0$ wave having possibly a reasonable large overlap with the J/ψ wave function. The first case requires either a very narrow or an unreasonably extended gaussian wave packet. There are indications that most probably the second case holds. First, the χ production

rate has been measured at one energy, 62 GeV. It is shown that half of the observed J/ψ's are coming from the γ-decay of the χ's. From the same ref. [12], one can infer the direct ψ' cross-section is about the same as the J/ψ one. Second, the theoretical considerations that we outline below indicate the initial $c-\bar{c}$ wave packet should have a non negligible size.

3.2 Theoretical indications

One can have indications on the wave packet using the most popular model for charm production, namely the gluon fusion model [13]. The corresponding transition matrix may be expressed in terms of the final momenta $\mathbf{p}_1', \mathbf{p}_2'$, for given x_1 and x_2, defined as usual [13]:

$$T = T(\mathbf{p}_1', \mathbf{p}_2', x_1, x_2). \tag{3.1}$$

We may use instead the total $c-\bar{c}$ momentum $\mathbf{P}_{\text{tot}}$ and the relative $c-\bar{c}$ momentum $\mathbf{p}_{\text{rel}}$

$$T = T(\mathbf{P}_{\text{tot}}, \mathbf{p}_{\text{rel}}, x_1, x_2). \tag{3.2}$$

The quantity

$$F(\mathbf{P}_{\text{tot}}, \mathbf{p}_{\text{rel}}) = \int \mathrm{d}x_1 \int \mathrm{d}x_2 \, G(x_1) \, G(x_2) \times |T(\mathbf{P}_{\text{tot}}, \mathbf{p}_{\text{rel}}, x_1, x_2)|^2 \, \delta(p) \tag{3.3}$$

is the average probability of producing a pair $c-\bar{c}$ with total and relative momenta $\mathbf{P}_{\text{tot}}, \mathbf{p}_{\text{rel}}$, the average being taken on the gluon distribution functions $G(x)$. The function $\delta(p)$ stands symbolically for energy-momentum conservation. The quantity $F(\mathbf{P}_{\text{tot}}, \mathbf{p}_{\text{rel}})$ may be interpreted as the (average) square of the $c-\bar{c}$ wave packet in $\mathbf{p}_{\text{rel}}$ space, when this pair is produced with the total momentum $\mathbf{P}_{\text{tot}}$. The function (3.3) is thus rather complicated. To have some idea about the wave packet, we numerically calculated the quantity

$$f(p_{\text{rel}}) = \int \mathrm{d}\Omega_{\text{rel}} \, F(\mathbf{P}_{\text{tot}} = 0, \mathbf{p}_{\text{rel}}), \tag{3.4}$$

which can be interpreted as the probability of finding the $c-\bar{c}$ pair at intermediate $x_F (= x_1 - x_2)$ with relative momentum of magnitude p_{rel}. Details are given elsewhere [14]. In other words, the quantity (3.4) can be interpreted as the squared modulus of the wave function in momentum space. If we identify the *initial* $c-\bar{c}$ wave packet with the *minimum* wave packet, i.e. the wave packet with the smallest r.m.s. radius, the r-representation of the initial wave packet will be given by the Fourier transform of the square root of $f(p_{\text{rel}})$. We show in Fig. 1 the function (3.4) and the squared modulus of the initial wave packet in r-space. Of course, by integrating over the direction of $\mathbf{p}_{\text{rel}}$, we have selected the $\ell = 0$ part of the wave function. Figure 1 shows that this $\ell = 0$ wave packet is definitely (but not dramatically) narrower than the J/ψ wave function.

Since both $f(p_{\text{rel}})$ and its r-representation are close to gaussian wave packets, we will use the latter as a convenient approximation.

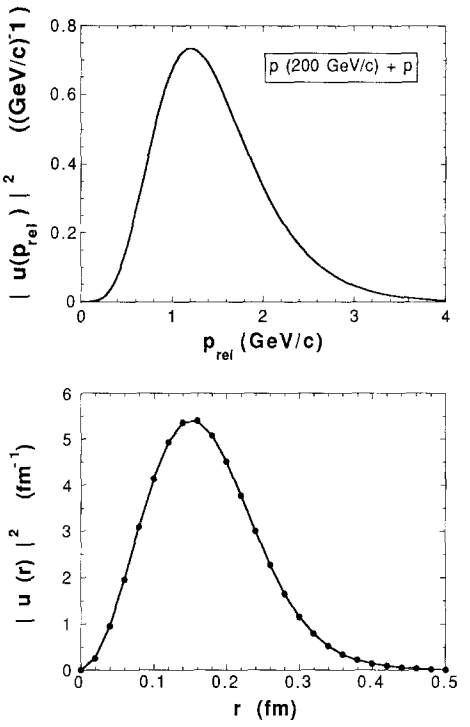

Fig. 1. Calculated $\ell = 0$ wave function, in momentum space (upper part, (3.4)) and in r-space (lower part), of the $c-\bar{c}$ pair formed in proton-proton collision at 200 GeV/c. See text for detail

In conclusion, these considerations support the idea that the small J/ψ content in the initial wave packet comes mainly from the rather small intensity of the $\ell = 0$ $c-\bar{c}$ component, the latter having possibly a reasonable overlap with the J/ψ wave function. For instance, the overlap of the normalized wave packet of Fig. 1 (scalar product squared) with a realistic J/ψ wave function is 0.44. To give an idea, a normalized gaussian wave packet

$$\psi = A \, \mathrm{e}^{-r^2/\sigma^2} = \frac{u(r)}{r} \frac{1}{\sqrt{4\pi}}, \tag{3.5}$$

with the same overlap, corresponds to $\sigma = 0.22$ fm. As a consequence, for solving (2.1), we will chose a gaussian wave function with σ between 0.19 fm and 0.25 fm, allowing so to study the sensitivity to the initial state.

4 Basic numerical results

We first present our results for the model described by (2.1)-(2.3). The quantities τ_p and τ_m should be viewed as the time spent in the plasma and in the mixed phase or transition region by the $c-\bar{c}$ pair, respectively, expressed in its proper rest frame. In a specific case, they can be related to the intrinsic properties of the plasma and of the transition, and to the kinematical conditions of the propagation of the $c-\bar{c}$ pair with respect to the medium. This relationship is discussed in Sect. 5.

If $\psi_{J/\psi}(\mathbf{r})$ is the static J/ψ wave function, we concentrate here on the quantity

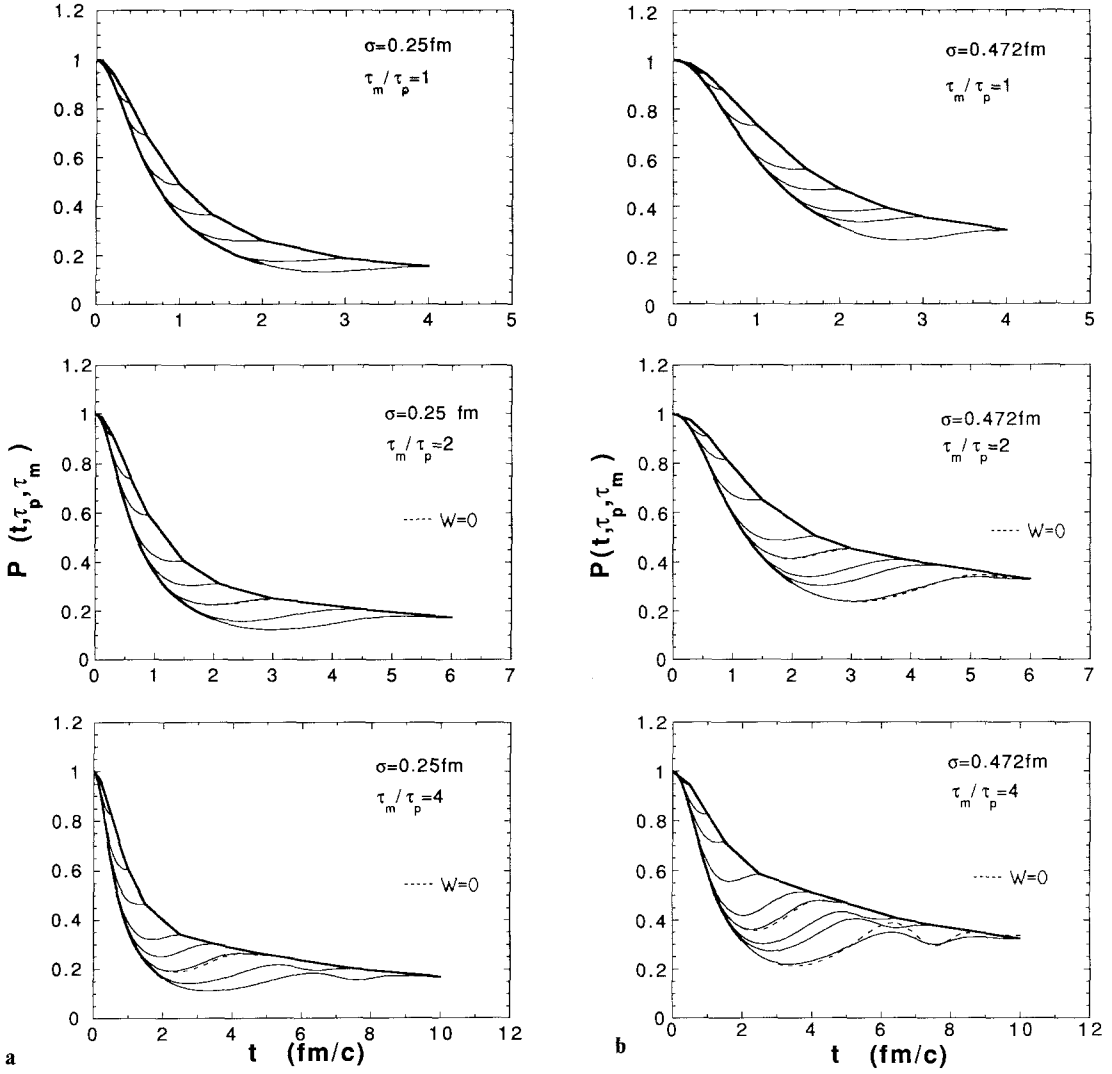

Fig. 2a, b. a Time evolution of the J/ψ probability (quantity (4.1)) for an initial wave function (3.5) with $\sigma = 0.25$ fm and for different values of the parameters τ_p, τ_m. In each group, the lower heavy line gives to the quantity $P(t, t, 0)$ for $t \leqq 2$ fm/c, i.e. the time evolution of the J/ψ probability in a pure plasma phase. In the upper graph, the narrow full lines give the quantity $P(t, \tau_p, \tau_m)$, for $\frac{\tau_m}{\tau_p} = 1$ and for various values of τ_p (0.1, 0.2, 0.3, 0.5, 0.7, 1, 1.5 and 2 respectively). The corresponding value of τ_p can be identified as the abscissa of the point where the narrow line departs from the lower heavy line. The upper heavy line merely represents the final values, i.e. the quantity $P(\tau_p + \tau_m, \tau_p, \tau_m)$ for a continuous variation of τ_p and the indicated $\frac{\tau_m}{\tau_p}$ ratio. Finally, the dotted lines give the results of calculations with a vanishing imaginary part. See text for detail. **b** Same for an initial wave packet (3.5) with $\sigma = 0.472$ fm

$$P(t, \tau_p, \tau_m) = \frac{|\langle \psi_{J/\psi}(r) | \psi(\mathbf{r}, t) \rangle|^2}{|\langle \psi_{J/\psi}(r) | \psi(\mathbf{r}, 0) \rangle|^2}, \tag{4.1}$$

for various values of τ_p and τ_m. The latter is given in Fig. 2 for several values of the ratio τ_m/τ_p and for various values of τ_p. It should be noticed that, for the range of parameters under study, (i) the J/ψ content always decreases in the plasma; (ii) the J/ψ content may decrease or increase in the mixed phase; (iii) the final J/ψ content is always smaller than initially.

The first result is expected since it is reminiscent of the case of a freely expanding gaussian wave packet. The second result may be qualitatively understood as follows. If the wave packet is very narrow when entering the mixed phase, it will mainly expand. If on the contrary it is broader than the J/ψ one, it may be compressed by the restoring confining potential and the overlap with the J/ψ may increase. This behaviour as many other features are well documented in [7], where the evolution of a wave packet in a restoring potential is extensively studied.

In Fig. 2, the effect of the coupling to the inelastic channels is also illustrated. It turns to be very negligible for the wave packets studied here. It may not be the case for other wave packets (see [7]). The physical reason may be understood as follows. Depending upon the value of $\tau_p + \tau_m$, the initial rather compact wave packet expands more or less importantly, but continuously. However the overlap with the J/ψ is mainly given by the small r part of the wave function ($\lesssim 1$ fm) and is thus not very much influenced by the absorption which roughly damps the

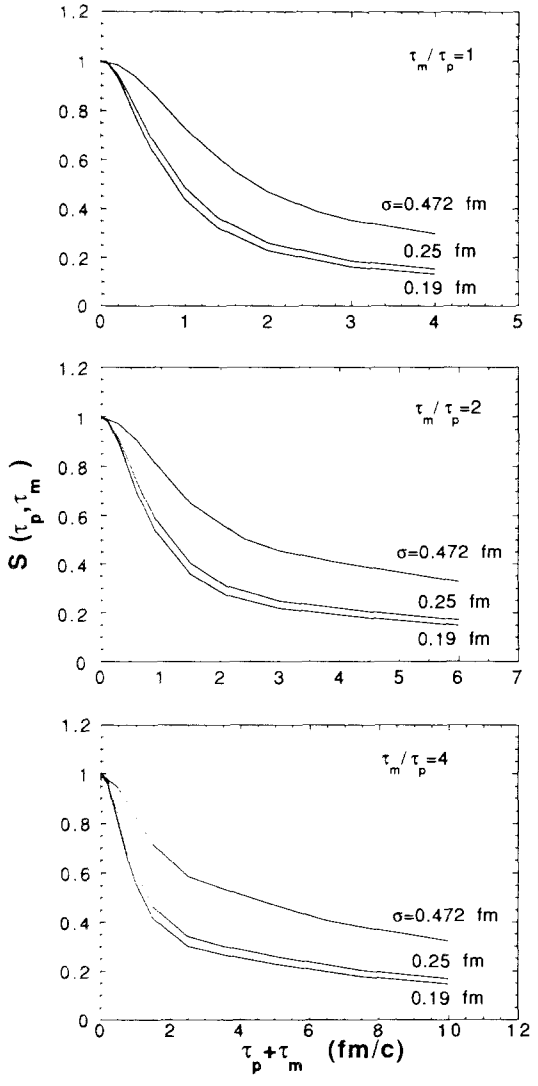

Fig. 3. Survival probability for the J/ψ, i.e. values of the quantities (4.2), as function of the total interaction time $\tau_p+\tau_m$, for various values of the ratio $\frac{\tau_m}{\tau_p}$. In each case, the calculations have been done with the initial wave packet (3.5), for the indicated values of the parameter σ. See text for detail

wave for $r > 1$ fm. A strong influence of the absorption would occur if the final small r part of the wave function resulted from the evolution of a wave packet entirely situated in the absorption zone at earlier times [7].

In Fig. 3, we display the final value of the J/ψ content, namely the quantity

$$S(\tau_p, \tau_m) = P(\tau_p + \tau_m, \tau_p, \tau_m) \tag{4.2}$$

for various values of the ratio τ_m/τ_p. This picture illustrates the sensitivity of the results upon the width of the initial gaussian wave packet. It turns out that the sensitivity is rather weak around the value of σ recommended in Sect. 2. It is also remarkable that if one starts with a value of $\sigma = 0.472$ fm, giving a r.m.s. radius equal to the one of the actual J/ψ, the relative depletion is much smaller. For $\sigma = 0.25$ fm, the quantity $S(\tau_p, \tau_m)$ is shown in Fig. 4 as iso-intensity curves. It can be seen that for a

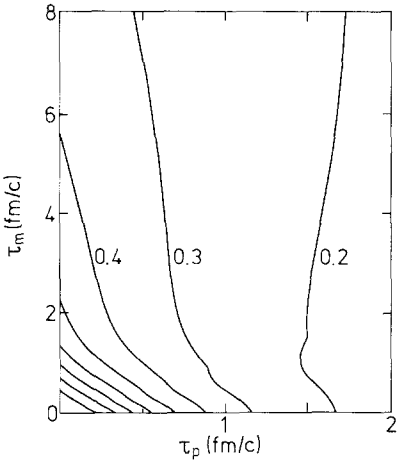

Fig. 4. Contour plot of the survival J/ψ probability (4.2). The values corresponding to the contour lines increase from 0.2 to 0.9 when going from left to right

given total time $\tau_p + \tau_m$, the largest final J/ψ abundance is obtained when all this time is spent in the mixed phase. For small τ_p and τ_m, one has roughly $S(0, \tau_m) \approx S\left(\tau_p = \frac{\tau_m}{2}, 0\right)$. This is qualitatively understood by noticing that the departure from the static charmonium potential in the mixed phase is on the average half the one prevailing in the plasma phase. For a large time spent in the plasma, the final J/ψ abundance does not depend very much upon the time spent in the mixed phase. Actually, a good numerical fit of the calculated value of S is given by

$$S(\tau_p, \tau_m) = \frac{\sqrt{1 + b\,\tau_g^c}}{1 + a\,\tau_g^2}, \tag{4.3}$$

with

$$\tau_g = \sqrt{\tau_p^2 + \tau_m^2}, \tag{4.4a}$$

$$a = 1.3748 - 0.6880\,\theta, \tag{4.4b}$$

$$b = 0.935\,\theta + 1.815, \tag{4.4c}$$

$$c = 4.835 - 3.116\,\sqrt{(\theta - 0.278)^2 + (0.40146)^2}, \tag{4.4d}$$

$$\theta = \operatorname{atan}\left(\frac{\tau_m}{\tau_p}\right), \tag{4.4e}$$

for $\sigma = 0.25$ fm. This parametrization is valid only in the range of variation of the variables indicated in Fig. 4.

In the following, we will concentrate on $S(\tau_p, 0)$ and $S(0, \tau_m)$ that we will rewrite by introducing characteristic times

$$S(\tau_p, 0) = \tilde{S}\left(\frac{\tau_p}{\tau_{J/\psi}^p}, 0\right), \tag{4.5a}$$

$$S(0, \tau_m) = \tilde{S}\left(0, \frac{\tau_m}{\tau_{J/\psi}^m}\right). \tag{4.5b}$$

There is no mathematical need to do so, but this will be helpful for introducing dimensionless physical parameters. Of course, $\tau^p_{J/\psi}$ and $\tau^m_{J/\psi}$ can be chosen arbitrarily, but we may fix them such that S is equal to 1/2 when $\tau_p = \tau^p_{J/\psi}$ or $\tau_m = \tau^m_{J/\psi}$, and think of them as the time spent in the plasma or the mixed phase, after which the J/ψ content of the wave packet is significantly reduced. With our choice for the initial wave packet, $\tau^p_{J/\psi} = 0.7$ fm/c and $\tau^m_{J/\psi} = 2$ fm/c.

5 J/ψ suppression

5.1 Introduction

In this section, we apply our model to the so-called J/ψ suppression in relativistic heavy-ion collisions. We will assume that the $c-\bar{c}$ pair is formed at the beginning of the plasma phase and that this phase lasts for some time. Our main goal is then to calculate the J/ψ survival probability for a given plasma scenario and to compare it to the quasi-classical approximation based on a J/ψ formation time τ_F, as introduced in previous analyses. According to this approximation, the $c-\bar{c}$ pair forms a J/ψ after τ_F only. If at that time, the $c-\bar{c}$ pair is sitting inside the plasma, it will be dissolved. If it is sitting outside, the J/ψ will survive. In order to disentangle the effects of the plasma itself, of its finite size and of the mixed phase, we will consider several plasma scenarios, including the case of an infinite plasma.

In this section, we will concentrate on the $p_\perp$ dependence of the quantity $\tilde{S}(\tau_p, \tau_m)$ for specific scenarios. We postpone the comparison with experimental data to the next section.

5.2 Infinite plasma of finite lifetime

We start with the simplest case of an infinite homogeneous plasma becoming suddenly an ordinary phase (no mixed phase) after a time t_p, seen in its rest frame. Let us consider a $c-\bar{c}$ pair formed at time $t=0$ with a momentum $p_\perp$, and let us call $F(p_\perp)$ the ratio of the probability of forming asymptotically ($t\to\infty$) a J/ψ to the initial probability. According (4.1), (4.2) and (4.5), the latter can simply be written as

$$F(p_\perp) = \tilde{S}\left(\frac{t_p}{\gamma_\perp \tau^p_{J/\psi}}, 0\right), \tag{5.1a}$$

with

$$\gamma_\perp = \frac{\sqrt{p_\perp^2 + M^2}}{M}, \tag{5.1b}$$

M being the mass of the $c-\bar{c}$ system, that we take as the J/ψ mass. The quantity $\tau_p = t_p/\gamma_\perp$ is the proper time spent in the plasma by the $c-\bar{c}$ pair of perpendicular momentum $p_\perp$. In this case, the $p_\perp$ dependence of the J/ψ survival follows a universal curve given in Fig. 5 and depending upon the dimensionless parameter

$$\xi^p_1 = \tau_p/\tau^p_{J/\psi}, \tag{5.2}$$

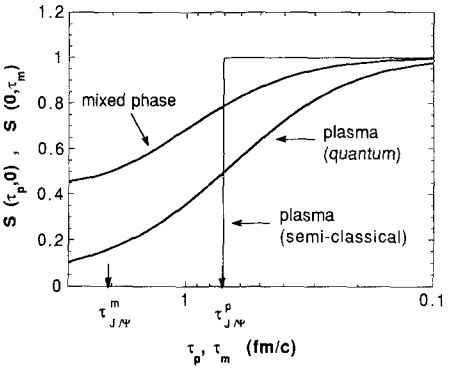

Fig. 5. Survival J/ψ probability in a pure plasma phase (lower curve) and in a mixed phase (upper curve). Note that the horizontal scale is increasing from right to left (in order to correspond to a $p_\perp$ scale increasing from left to right). The values of $\tau^m_{J/\psi}$ and $\tau^p_{J/\psi}$ are indicated by the arrows on the horizontal scale. The step function curve gives the semi-classical approximation (5.4) for $\tau_F = \tau^p_{J/\psi}$

i.e the ratio of the proper time spent inside the plasma to the typical "decay" time of the J/ψ component. If one focuses on the $p_\perp$ range extending from 0 to M, one may be interested in the quantity

$$F(M) - \mathrm{F}(0) = \tilde{S}\left(\frac{t_p}{\sqrt{2}\,\tau^p_{J/\psi}}, 0\right) - \tilde{S}\left(\frac{t_p}{\tau^p_{J/\psi}}, 0\right)$$
$$\approx \tilde{S}\left(0.71\,\frac{t_p}{\tau^p_{J/\psi}}, 0\right) - \tilde{S}\left(\frac{t_p}{\tau^p_{J/\psi}}, 0\right). \tag{5.3}$$

One clearly sees from Fig. 5 that this quantity cannot be larger than ~ 0.2. (Graphically, (5.3) is given by the difference of the ordinates of two points whose abscissa are separated by a constant length in Fig. 5, whatever the value of $\frac{t_p}{\tau^p_{J/\psi}}$ is). Furthermore, if $F(M) \approx 1$ (which can occur if t_p is very small), (5.3) is also very small. This is illustrated by Fig. 6, which shows the function $F(p_\perp)$ for $t_p = 0.5$ fm/c. This figure also shows the relative insensitivity upon the width of the initial wave packet (around $\sigma \sim 0.2$ fm). Our calculated function $F(p_\perp)$ is compared in this case with the prediction of the semi-classical model, which is

$$F_{\mathrm{SC}}(p_\perp) = \theta\left(\tau_F - \frac{t_p}{\gamma_\perp}\right)$$
$$= \theta\left(1 - \frac{t_p}{\gamma_\perp \tau_F}\right) = \tilde{S}_{\mathrm{SC}}\left(\frac{t_p}{\gamma_\perp \tau_F}\right), \tag{5.4}$$

where $\theta(x)$ is equal to unity if $x > 0$ and vanishes otherwise.

This ideal example singles out the spectacular effect of quantum mechanics, which smoothens the function $F(p_\perp)$ efficiently. Let us notice that both (5.1) and (5.4) can be put into the form

$$F(p_\perp) = f\left(\frac{t_p}{\tau_x \gamma_\perp}\right) = f\left(\frac{\tau_p}{\tau_x}\right), \tag{5.5}$$

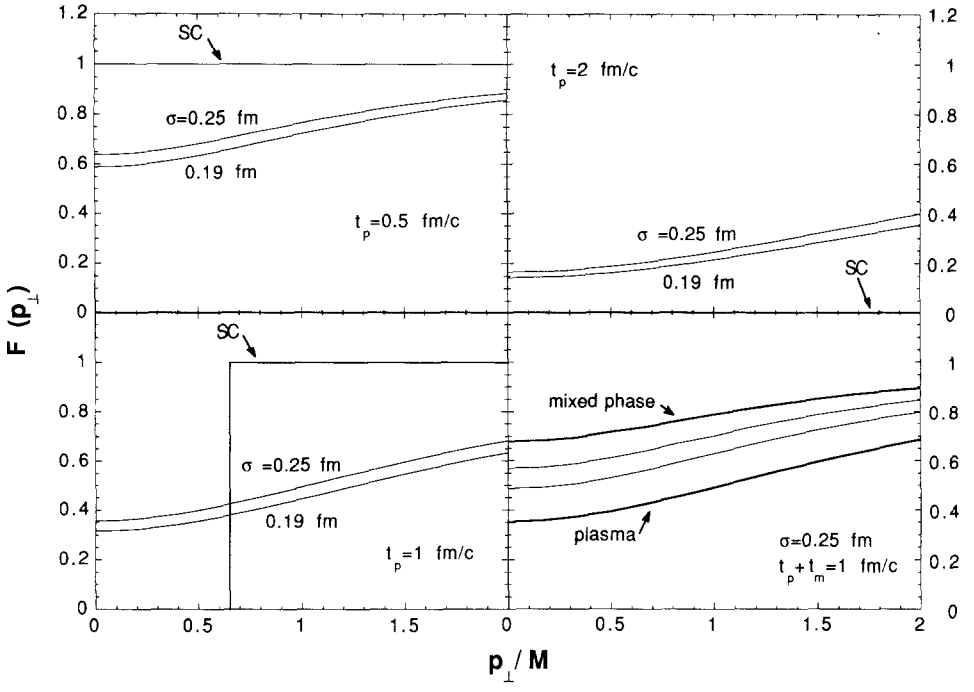

Fig. 6. Transverse momentum distribution of the J/ψ survival probability for an infinite homogeneous plasma of finite lifetime $t_p = 0.5$ fm/c (upper left), 1 fm/c (lower left) and 2 fm/c (upper right), respectively. The calculation has been done with the initial wave packet (3.5) and for $\sigma = 0.19$ fm and 0.25 fm. The curves indicated SC correspond to the semi-classical approximation (5.4) for τ_F taken equal to $\tau^p_{J/\psi}$. The quantity M is the mass of the J/ψ. The lower right part of the figure corresponds to the case where the infinite plasma transforms into a mixed phase after time t_p, which in turns transforms into a hadronic gas at time $t_p + t_m$, equal to 1 fm/c. The curves correspond to $t_p = 0$, 0.25, 0.5 and 1, respectively, when going from top to bottom

exhibiting a single relevant physical parameter. In our picture, τ_x characterizes the decrease of the J/ψ intensity inside the plasma, whereas in the semi-classical picture, it is to be identified to the so-called formation time. The basic difference between the two approaches is that the function f may display strong variations in the semi-classical picture, whereas it is rather smooth in our picture.

We may also consider the simple case of an infinite plasma phase of vanishing lifetime giving rise (at $t=0$) to an infinite mixed phase of duration time t_m (in its rest frame). The quantity $F(p_\perp)$ will then be given by

$$F(p_\perp) = S\left(0, \frac{t_m}{\gamma_\perp}\right) = \tilde{S}\left(0, \frac{t_m}{\gamma_\perp \tau^m_{J/\psi}}\right) = \tilde{S}(0, \xi_1^m), \tag{5.6}$$

where the function $S(0, x)$ is shown in Fig. 5. For $t_m = t_p$, the reduction is larger in a pure plasma phase than in the mixed phase. Since $S(x+y, 0) < S(x, y) < S(0, x+y)$ (see Fig. 4), for a given total interaction time, the reduction will always be the largest in the plasma phase and the smallest for the mixed phase and intermediate between these two extremes for a plasma phase followed by a mixed phase. This is shown in Fig. 6. This property holds in all the cases below. We henceforth will only show the pure plasma and the pure mixed phase cases.

5.3 *Finite size plasma of infinite lifetime*

In order to simplify the calculations, we will consider an homogeneous cylindrical plasma of transverse radius R_0, but of inifinite length and of infinite lifetime. Since we are considering transverse motion and since the plasma which is possibly formed in heavy ion collisions is likely of elongated shape, neglecting end effects is justified in first approximation.

Following [15], we consider that a $c-\bar{c}$ pair may be formed anywhere in the plasma with a probability $\rho(r)$, depending only upon the radial distance (in cylindrical coordinates) and with a direction of $\mathbf{p}_\perp$ at random.

If we first assume that the plasma is not surrounded by a mixed phase (i.e. the $c-\bar{c}$ is free as soon as it leaves the plasma), the function $F(p_\perp)$ may be written as

$$F(p_\perp) = 2\pi \int_0^{R_0} \rho(r) r \, dr \int_0^{\pi} \frac{d\theta}{\pi} \tilde{S}\left(\frac{d(r,\theta)}{\beta_\perp \gamma_\perp \tau^p_{J/\psi}}, 0\right), \tag{5.7a}$$

where θ is the angle between the vectors $\mathbf{p}_\perp$ and $\mathbf{r}$ (perpendicular to the cylindrical axis) and where d is the distance between $\mathbf{r}$ and the surface, i.e. the (perpendicular) distance travelled inside the plasma. The distribution $\rho(r)$ is normalized according

$$2\pi \int_0^{R_0} \rho(r) r \, dr = 1. \tag{5.7b}$$

Introducing the reduced variable $z = d/R_0$, we may rewrite (5.7a) as

$$F(p_\perp) = 2 \int_0^{R_0} \rho(r) r \, dr \int_0^{\pi} d\theta \int_0^{2} dz \, \delta\left(z - \frac{d(r,\theta)}{R_0}\right) \times \tilde{S}\left(\frac{z R_0}{\beta_\perp \gamma_\perp \tau^p_{J/\psi}}, 0\right), \tag{5.8}$$

since d always lies between 0 and $2R_0$, or as

$$F(p_\perp) = \int_0^{2} dz \, g(z) \tilde{S}\left(\frac{z R_0}{\beta_\perp \gamma_\perp \tau^p_{J/\psi}}, 0\right). \tag{5.9}$$

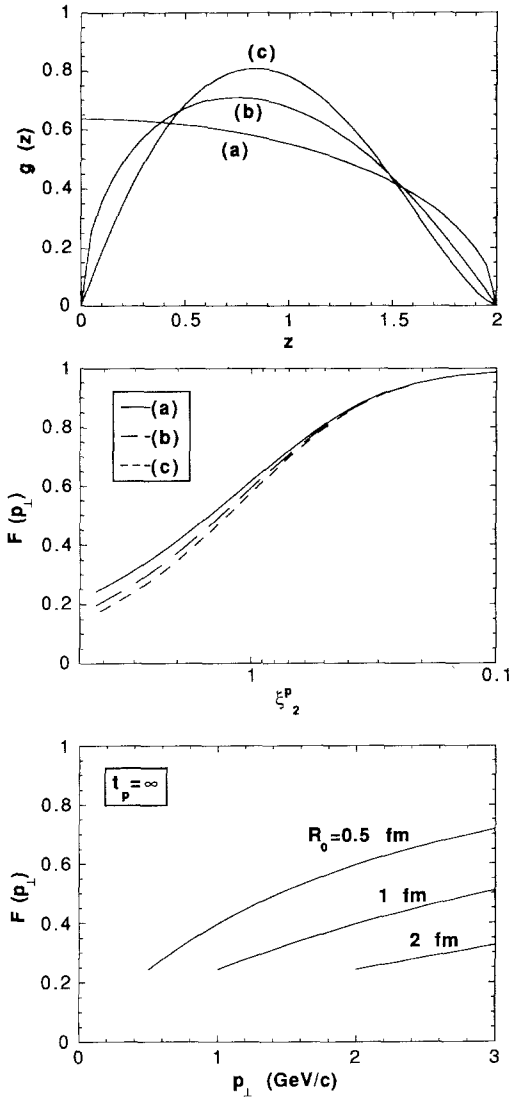

Fig. 7. Case of a finite size plasma with infinite lifetime (see Sect. 5.3). The upper part gives the distribution of the path lengths (divided by the radius) travelled by the $c-\bar{c}$ pairs inside the plasma, for three different distributions, (a), (b), (c), of the $c-\bar{c}$ pairs at initial time, corresponding to (5.12a), (5.12b) and (5.12c), respectively. The middle part gives the J/ψ survival probability in function of the parameter ξ_2^p (5.11) for the three distributions mentioned above. The lower part gives the $p_\perp$-distribution for various values of the radius R_0 of the plasma and for the distribution (5.12a)

The function

$$g(z)=2\int_0^{R_0}\rho(r)\,r\,\mathrm{d}r\int_0^{\pi}\mathrm{d}\theta\,\delta\left(z-\frac{d(r,\theta)}{R_0}\right) \tag{5.10}$$

simply represents the distribution of the distances to be travelled in order to get out of a circle when one is sitting at a distance r of the centre, with a probability $\rho(r)$, and one is choosing a direction at random. For a given distribution $g(z)$, the quantity $F(p_\perp)$ is a function of the single parameter

$$\xi_2^p=\frac{R_0 M}{p_\perp \tau_{J/\psi}^p}=\frac{\tau_{\mathrm{esc}}}{\tau_{J/\psi}^p}, \tag{5.11}$$

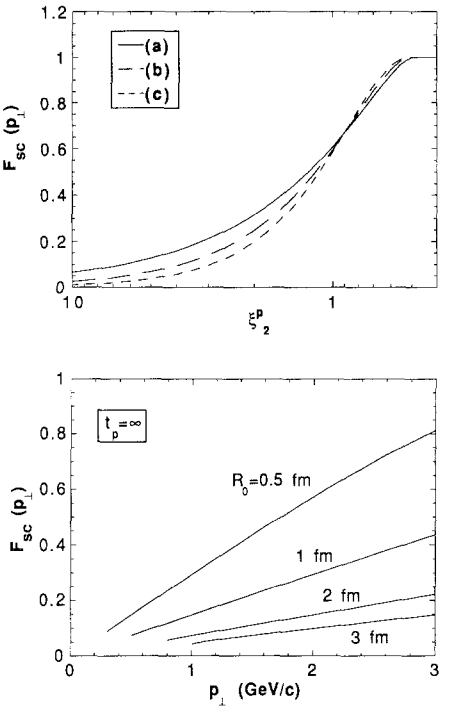

Fig. 8. Semi-classical approximation for the cases investigated in the middle and lower parts of Fig. 7, assuming $\tau_F=\tau_{J/\psi}^p$. See text for detail

where τ_{esc} is the time necessary for escaping from the center of the plasma. Figure 7 shows the function $g(z)$ for three different distributions $\rho(r)$, namely

$$\rho(r)=\frac{1}{\pi R_0^2}, \tag{5.12a}$$

$$\rho(r)=\frac{3}{2\pi R_0^2}\sqrt{1-r^2/R_0^2}, \tag{5.12b}$$

$$\rho(r)=\frac{2}{\pi R_0^2}(1-r^2/R_0^2), \tag{5.12c}$$

and the corresponding distributions $F(p_\perp)$ as expressed in terms of the variable ξ_2^p, and in terms for $p_\perp$ for different values of R_0. Note that here $F(0)$ is always equal to zero, since an infinitely slow pair will spend an infinite time in the plasma. This can occur only in scenarios with an infinite plasma lifetime.

In Fig. 8, we show the function $F_{\mathrm{SC}}(p_\perp)$ when calculated within the semi-classical approximation, i.e. with a function $\tilde{S}_{\mathrm{SC}}$ given by (5.4). Note that here quantum mechanics introduces a much more reduced effect compared to the case of Fig. 6. This, of course, comes from the smoothing through the distribution function $g(z)$. Note also the rough insensitivity of both $F(p_\perp)$ and $F_{\mathrm{SC}}(p_\perp)$ on the distribution function $\rho(r)$.

5.4 Finite size plasma of finite lifetime

We consider now a plasma with the same geometry as above, but which transforms suddenly in a hadronic phase after a time t_p. Mathematically, $F(p_\perp)$ is now given by

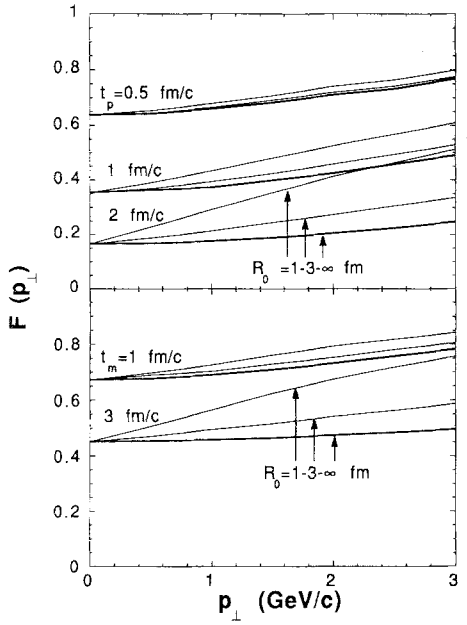

Fig. 9. Perpendicular momentum dependence of the J/ψ survival probability in the case of a finite size plasma with a finite lifetime t_p (upper part of the figure). Calculations have been carried with $t_p = 0.5$, 1 and 2 fm/c, respectively. For each case, the upper, middle and lower curves correspond to a radius $R_0 = 1$ fm, 3 fm and infinity, respectively. The lower part of the figure corresponds to the case of a finite size mixed phase with a finite lifetime. The calculations have been carried out with the initial $c-\bar{c}$ density distribution (5.12a). See text for detail

$$F(p_\perp) = \int_0^2 \mathrm{d}z\, g(z)\, \tilde{S}(\min[\xi_1^p, z\,\xi_2^p], 0), \tag{5.13}$$

where ξ_1^p and ξ_2^p have been defined in (5.2) and (5.11), respectively. The results are then given in Fig. 9. The effect of the finite size appears less important than the effect of the finite lifetime in the indicated range of values for the parameters $p_\perp, R_0, \tau^p_{J/\psi}$. In Fig. 9, we also show the values of $F(p_\perp)$, given this time by

$$F(p_\perp) = \int_0^2 \mathrm{d}z\, g(z)\, \tilde{S}(0, \min[\xi_1^m, z\,\xi_2^m]), \tag{5.14}$$

with

$$\xi_1^m = \frac{t_m}{\gamma_\perp \tau^m_{J/\psi}}, \qquad \xi_2^m = \frac{\tau_{\mathrm{esc}}}{\tau^m_{J/\psi}}, \tag{5.15}$$

corresponding to a finite size mixed phase becoming a hadron phase in a time t_m. The function $F(p_\perp)$ so obtained is always larger than the corresponding one of the plasma, for $t_m = t_p$, and can be considered as an upper limit, if one starts with a plasma evolving in a mixed phase and in a hadronic phase in the same time span.

5.5 *Contracting plasma*

We now consider the case where we start with an homogeneous plasma of cylindrical symmetry (and infinite axis) transforming at its surface into a hadronic phase. We consider that the interface is a cylindrical surface with a radius $R(t)$ going continuously from the initial radius R_0 to zero (corresponding to the disappearance of the plasma), in a finite time t_p. In this case, (5.7) becomes

$$F(p_\perp) = 2\pi \int_0^{R_0} \rho(r)\, r\,\mathrm{d}r \int_0^\pi \frac{\mathrm{d}\theta}{\pi} \int_0^{t_p} \times \delta\left(d\left(r, \theta, \frac{p_\perp}{M\gamma_\perp}, t\right) - R(t)\right) \times \left|\frac{\partial(d-R)}{\partial t}\right| \tilde{S}\left(\frac{t}{\gamma_\perp \tau^p_{J/\psi}}, 0\right) \mathrm{d}t, \tag{5.16}$$

where d is the distance of the axis of a $c-\bar{c}$ pair at time t, which has been initially created at a distance r and travelling with a perpendicular momentum $p_\perp$ in the direction θ:

$$d^2\left(r, \theta, \frac{p_\perp}{M\gamma_\perp}, t\right) = r^2 + \frac{p_\perp^2 t^2}{M^2\gamma_\perp^2} + \frac{2rp_\perp t}{M\gamma_\perp}\cos\theta. \tag{5.17}$$

We may rewrite (5.16) with the reduced variables $x = r/R_0$, $\zeta = d/R_0$

$$F(p_\perp) = 2\int_0^1 \tilde{\rho}(x)\, x\,\mathrm{d}x \int_0^\pi \mathrm{d}\theta \int_0^{t_p} \times \delta\left(\zeta\left(x, \theta, \frac{p_\perp}{MR_0\gamma_\perp}, t\right) - \frac{R(t)}{R_0}\right) \times \left|\frac{\partial\left(\zeta - \frac{R(t)}{R_0}\right)}{\partial t}\right| \tilde{S}\left(\frac{t}{\gamma_\perp \tau^p_{J/\psi}}, 0\right) \mathrm{d}t, \tag{5.18}$$

where $\tilde{\rho}$ is normalized as ρ and thus depends upon x only. We below consider three models for $R(t)$, namely

$$R(t) = R_0\,\theta\left(1 - \frac{t}{t_p}\right), \tag{5.19a}$$

$$R(t) = R_0\left(1 - \left(\frac{t}{t_p}\right)^2\right)^{1/2}, \tag{5.19b}$$

and

$$R(t) = R_0\left(1 - \left(\frac{t}{t_p}\right)\right). \tag{5.19c}$$

As an example, for a linear variation, one obtains, introducing $y = \frac{t}{t_p}$

$$F(p_\perp) = 2\int_0^1 \tilde{\rho}(x)\, x\,dx \int_0^\pi d\theta \int_0^1 \times \delta\left(\zeta\left(x,\theta,\frac{p_\perp t_p}{R_0 M y_\perp}, y\right) - 1 + y\right) \times \left|\frac{\partial\zeta}{\partial y} + 1\right| \tilde{S}\left(\frac{y t_p}{y_\perp \tau^p_{J/\psi}}, 0\right) dy. \quad (5.20)$$

Whatever the function $R\left(\frac{t}{t_p}\right)$ is, the distribution depends upon the two dimensionless parameters ξ_1^p and ξ_2^p introduced previously. For the purpose of illustration, we can take the limit $R_0 \to \infty$. This corresponds to the unphysical case of an interface coming from infinity with infinite speed. Note that mathematically, this is equivalent to having a finite R_0, but an infinite mass M of the $c-\bar{c}$ pair. The physical situation close to this limit corresponds to an interface travelling much faster than the pair $\left(\frac{R_0}{\tau_p} \gg \frac{p_\perp}{M y_\perp}\right)$. In that limit, the distribution depends upon the single parameter, ξ_1^p. The results are plotted in Fig. 10 as function of this parameter (the choice of the scale corresponds to a monotonously increasing $p_\perp$). In the same figure, the results for the semi-classical model (with $\tilde{S}_{SC}$ of (5.4)) are also displayed. Once again the $p_\perp$ -dependence is much smoother in the quantum case. Furthermore, one may notice that the smoother the variation of $R(t)$ is (from (5.19a) to (5.19c)), the smaller the suppression is and the smoother the function $F(p_\perp)$ is.

The results for a finite initial volume (finite R_0) are given in Fig. 11, both for the quantum and the semi-classical models. Once again, the results are similar, but

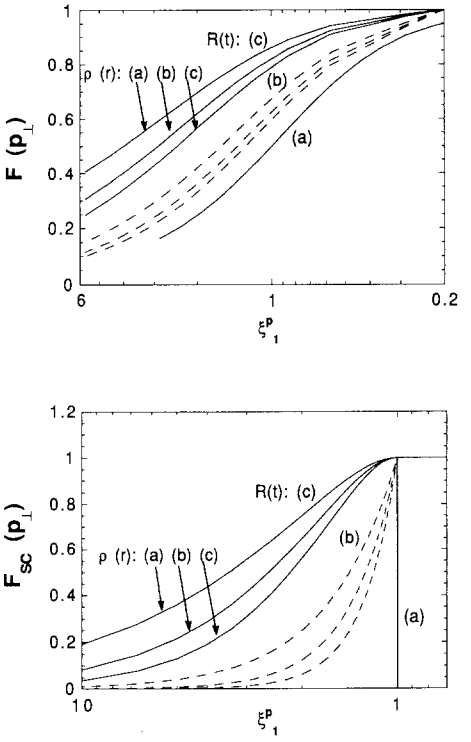

Fig. 10. Perpendicular momentum dependence of the J/ψ survival probability in the case of a "shrinking" plasma, for three time dependences of the plasma radius $R(t)$, given by (5.19a), (5.19b) and (5.19c) respectively and for three possible distributions of the $c-\bar{c}$ pair density $\rho(r)$ inside the plasma, corresponding to (5.12a), (5.12b) and (5.12c), respectively. The calculation corresponds to the limiting case of an initial infinite radius. The upper part of the figure displays the quantum results, versus the parameter ξ_1^p (5.2). The lower part corresponds to the semi-classical results, as functions of the same quantity as in the upper part, where the quantity τ_F has been substituted to $\tau^p_{J/\psi}$. See text for detail

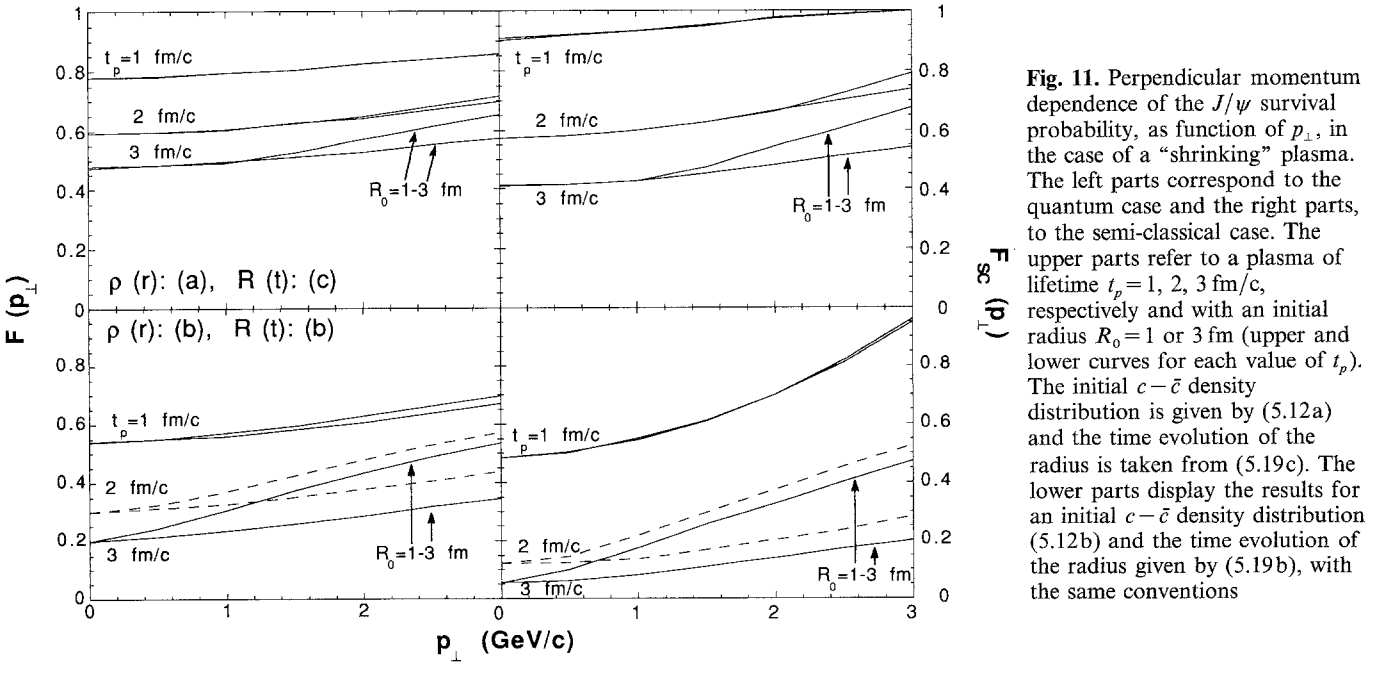

Fig. 11. Perpendicular momentum dependence of the J/ψ survival probability, as function of $p_\perp$, in the case of a "shrinking" plasma. The left parts correspond to the quantum case and the right parts, to the semi-classical case. The upper parts refer to a plasma of lifetime $t_p = 1, 2, 3$ fm/c, respectively and with an initial radius $R_0 = 1$ or 3 fm (upper and lower curves for each value of t_p). The initial $c-\bar{c}$ density distribution is given by (5.12a) and the time evolution of the radius is taken from (5.19c). The lower parts display the results for an initial $c-\bar{c}$ density distribution (5.12b) and the time evolution of the radius given by (5.19b), with the same conventions

smoother in the quantum case, so much that there is no strong variation of $F(p_\perp)$ between $p_\perp = 0$ and $p_\perp = 3$ GeV/c for any of the values of R_0 and of t_p indicated on the figure. However, one may notice a significant variation with t_p. Mathematically, this comes from the fact that, in the domain of variation of the parameters $p_\perp$, R_0, t_p investigated here, the function $F(p_\perp)$ is more rapidly varying with ξ_1^p than with ξ_2^p. Physically, and in illustrative words, one may say that the J/ψ survival observed in Fig. 11 is due more to the shrinking of the surface (variation with t_p) than to the escape from the plasma (variation with $p_\perp$).

5.6 Contracting mixed phase

In order to contrast with the previous scenario, we consider (with the same geometry) the case of a mixed phase changing into a hadronic phase with an interface moving from R_0 to 0 in a time t_m. Mathematically, this corresponds to replacing $\tilde{S}\left(\frac{t}{\gamma_\perp \tau^p_{J/\psi}}, 0\right)$ in (5.16) and following ones by $\tilde{S}\left(0, \frac{t}{\gamma_\perp \tau^m_{J/\psi}}\right)$. The results are shown in Fig. 12, both for infinite and finite R_0. Comparing the upper parts of Figs. 10 and 12 respectively, one sees, as expected, that the suppression is smaller in the mixed phase, practically in the ratio given by the one of the

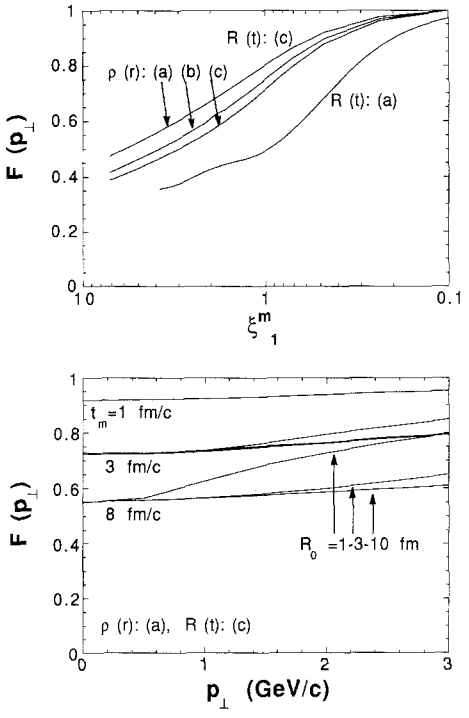

Fig. 12. Upper part: same as the upper part of Fig. 10a for a "shrinking" mixed phase. The quantity ξ_1^m is defined in (5.15). Lower part: perpendicular momentum dependence of the J/ψ survival for a "shrinking" mixed phase of duration $t_m = 1$, 3, and 8 fm/c and of initial radius $R_0 = 1$, 3 and 10 fm, respectively. The initial $c-\bar{c}$ density distribution is given by (5.12a) and the time evolution of the radius, by (5.19c). For $t_m = 1$ fm/c, the curves for the three different values of R_0 are indistinguishable

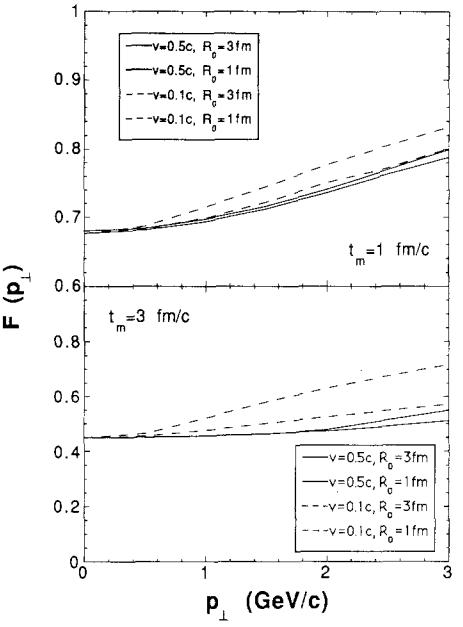

Fig. 13. Perpendicular momentum distribution of the J/ψ survival probability for an expanding mixed phase (see Sect. 5.7). The initial radius R_0, the velocity v of the linearly growing radius and the duration time of the mixed phase t_m are indicated

functions $\tilde{S}(x, 0)$ and $\tilde{S}(0, x)$ (see Fig. 5). Comparing the lower part of Fig. 12 with the upper left part of Fig. 11, one notices that the variation with t_m in the mixed phase scenario is less important than with t_p in the plasma scenario.

5.7 Expanding mixed phase

As a last illustrative case, we consider a finite mixed phase that expands for a while (t_m) and then suddenly transforms into a hadronic phase. The results are shown in Fig. 13, for several values of the initial radius R_0, of the expanding velocity and for two values of t_m. The $p_\perp$-dependence is rather flat, and the average value of $F(p_\perp)$ decreases with increasing t_m.

5.8 Discussion

The difference between the quantum-mechanical treatment and the semi-classical one is intrinsically important as demonstrated by Fig. 5. We here discuss scenarios involving the plasma only, since the semi-classical approximation has been defined in this context only. Quantum-mechanical and semi-classical treatments roughly yield the same results when the proper time spent in the plasma is either very short or very long compared to $\tau^p_{J/\psi}$ (provided one identifies τ_F with $\tau^p_{J/\psi}$). This intrisic difference between the results of the quantum and semi-classical approaches can be observed in the scenarios of an infinite plasma with finite lifetimes illustrated in Fig. 6. On the contrary, it may be obscured and very much attenuated in more realistic scenarios, which introduce some kinds of average over short, long and intermediate proper times spent by the $c-\bar{c}$ pairs inside the plasma. This is

particularly true for the finite size plasma of infinite lifetime investigated in Sect. 5.3 and illuminated by the comparison of the middle and lower graphs in Fig. 7 on the one hand with the two graphs in Fig. 8 on the other hand. The difference between the results of the two treatments is still remarkable for the scenario involving a "shrinking" plasma (Sect. 5.4) for a variation of $R(t)$ which is not smooth, like the one given by (5.19), and that for an "infinite" initial radius (see Fig. 10) as well as for the finite case (see Fig. 11).

The main effect of the quantum treatment is a flattening of the $p_\perp$ dependence in the 0–3 GeV/c range. As we already explained in Sect. 5.3, this range in $p_\perp$ translates in a small relative variation in the time spent in the plasma. A strong variation in $p_\perp$ may be obtained semi-classically when the domain of variation in proper time encompasses τ_F, in contradistinction with the quantum-mechanical case (see Fig. 5). The only scenario in which the quantum treatment yields a large variation in $p_\perp$ is the one involving a plasma of finite size with an infinite lifetime, because it involves very short (in large $p_\perp$ and small radii) and very long (for $p_\perp = 0$) times spent in the plasma.

One may qualitatively do the same discussion for mixed phase scenarios, introducing a semi-classical "formation time" and a semi-classical survival function $\tilde{S}_{SC} = \theta\left(1 - \frac{\tau_m}{\tau_F}\right)$ quite similarly to the plasma case.

We have seen that the presence of a mixed phase gives systematically, for the same total evolution time, less suppression.

When considering the plasma alone, the most realistic scenario is the one of Sect. (5.5). However, it is expected that the plasma "evaporates" in a mixed phase which is presumably first expanding and later on disappears. In the absence of any serious quantitative indications on this scenario, we gave, for the purpose of illustration, the results obtained for an expanding mixed phase. The main result is that, if this mixed phase lasts for some time, the suppression will be significantly increased.

6 Comparison with experiment

The NA38 collaboration [16, 17] basically produces two kinds of experimental data concerning the J/ψ suppression in relativistic heavy ion collisions: the suppression versus the transverse energy and suppression versus the perpendicular momentum. The theoretical description of the second one demands a model for the J/ψ evolution and a model for the plasma evolution. For the first kind of data, one needs in addition a theoretical model for the production of transverse energy. Since this introduces an additional uncertainty, we will concentrate here on the $p_\perp$ distribution only.

The comparison of our results with the experimental data on the $p_\perp$-distribution of the J/ψ suppression is nevertheless made difficult by several facts:

(1) what is in fact measured in [17] is the ratio of the J/ψ over continuum ratio for the bin of highest transverse energy ($E_T > 78$ GeV) and the one for the bin of lowest transverse energy ($E_T < 34$ GeV). It seems reasonable [18] to consider that the continuum does not change (this is in keeping with the absence of significant A-dependence in the Drell-Yan yield observed in [19]). Therefore, what is basically measured is the ratio of the J/ψ yield for high and low transverse energy. We will assume that the J/ψ suppression is negligible for peripheral collisions and identify the latter with the low transverse energy events. Although this seems acceptable, we should emphasize that there is no formal proof of this statement. Within this assumption, the measurements can be considered as giving the J/ψ suppression in central collisions, the latter being identified with the high transverse energy events.

(2) Our results of Sect. 5 deal with the evolution of the $c-\bar{c}$ pair after its production, assuming that its transverse momentum is not modified. This seems reasonable in view of the large mass of the J/ψ and of the probable expansion of the system (nor only the plasma). However, the initial state interaction (i.e. prior to $c-\bar{c}$ formation) may influence the observed $p_\perp$-distribution. The gluons prior to fusion are expectedly scattered more in central collisions than in peripheral collisions. This problem has recently been investigated by Gupta and Satz [20]. Fortunately enough, they corrected the data for these initial state interactions. We can so directly compare our results with the corrected data.

(3) The observed J/ψ's are not only coming from initial $\ell = 0$ $c-\bar{c}$ pairs. Some of them are coming from χ resonances. We will disregard first this aspect and comment on it later on.

The remarkable feature of the $S-U$ data of [17] is that the J/ψ suppression curve appears quite flat, after correction of [20] for initial state interaction, in the 0–3 GeV/c range. This is to be compared with our results with the quantum-mechanical treatment, which produces the same effect, except for the very special scenario of Sect. 5.3 with a small radius ($\lesssim 1$ fm) and very large (infinite) lifetime.

It is clear from Sect. 5 that there should be no difficulty to find a plasma scenario and numerical values of the parameters reproducing the data of Fig. 14. We do not intend to produce here the best fit, but we will roughly determine the values of the parameters for the most realistic scenarios. First of all, we should not consider the radius of the plasma as a free parameter, but more or less given by the radius of the incident nucleus, say 3 fm. Let us consider first pure plasma scenarios (no mixed phase). If we have a plasma of fixed radius and finite lifetime (see Fig. 9, top), the data are reproduced with a short lifetime ($t_p \approx 0.6$ fm/c, see Fig. 14). If we consider the scenario of a shrinking plasma (see Fig. 11), the data are reproduced with a lifetime of $t_p \approx 2$ fm/c if it shrinks with the time dependence (5.19c) (see Fig. 14) or of $t_p \approx 1$ fm/c, with (5.19b). It is to be noticed that in this scenario, the data cannot be reproduced by the semi-classical formalism, with reasonable values of the parameters at least. We should also underline that in these two scenarios, the results would be largely insensitive to a modification of the parameter R_0.

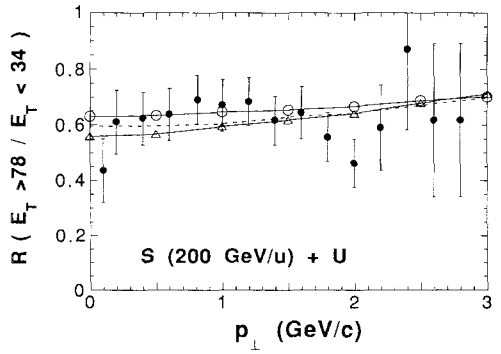

Fig. 14. The heavy dots with the error bars give the values of the ratio R, as defined and measured by the NA38 collaboration [16, 17] and corrected by [20] to get rid of the initial state interactions. The smooth curves correspond to our calculations for three scenarios: finite plasma of finite lifetime (triangles, $R_0 = 3$ fm, $t_p = 0.6$ fm/c, see Fig. 9), "shrinking" plasma (dotted line, $R_0 = 3$ fm, $t_p = 2$ fm/c, see Fig. 11, $\rho(r)$ given by (5.12a)) and "shrinking" mixed phase (open dots, $R_0 = 3$ fm, $t_m = 5$ fm/c, see Fig. 12)

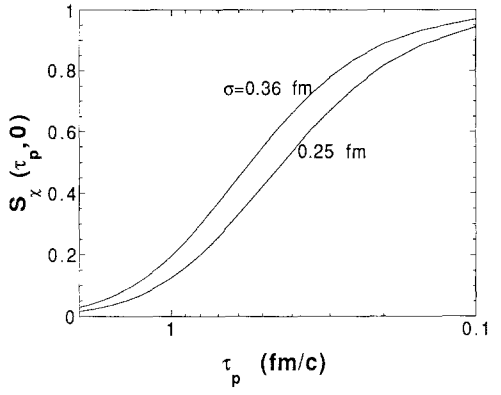

Fig. 15. Survival probability for a χ state inside a plasma (see Sect. 6), for two values of the parameter σ

Let us now comment on scenarios with a mixed phase. It is obviously more realistic to introduce this phase. However, very little is known about it. According to recent investigations, based on dynamical models for the phase transition [21, 22], this phase would last for a rather long time (several fm/c's). If we consider a finite size plasma, becoming a mixed phase, but keeping the same geometry, it is clear from Fig. 9 (bottom) that a global suppression of ~ 0.6 can only be obtained with a short total interaction time. If we consider the scenarios with mixed phase only, the data can easily been reproduced in a finite and constant size mixed phase (see Fig. 9) disappearing after a time $t_m \approx 1.5$ fm/c as well as in a "shrinking" mixed phase (see lower part of Fig. 12 and Fig. 14) with a lifetime $t_p \approx 5$–6 fm/c and with an evolution profile of type (5.19c). The expanding mixed phase of Fig. 13 is probably not very relevant at the SPS energy. It is clear however that there is no difficulty to find values of the parameters in order to agree with the data.

One has to keep in mind that a large fraction of the J/ψ's comes from the χ-decays [12]. This presumably does not affect our conclusions. Indeed, we have calculated the χ suppression in the plasma. This is illustrated in Fig. 15. We used a radial wave function of the type $u(r) \propto r^2 \exp\left(-\frac{r^2}{\sigma^2}\right)$, with different values of σ. The curves are very similar to the J/ψ one (see Fig. 5) and rather insensitive to the parameter σ. Of course, one should in principle follow the evolution of the χ in the various scenarios. But it is clear that the change will not be important. These considerations are however indicative only, since we did not calculate the initial χ wave function as for the J/ψ, we neglected the spin effects and we have no indication for the value of $W(r)$ in this channel [6].

7 Discussion, conclusion

We have investigated here the effect on the internal structure of the $c-\bar{c}$ pair on the J/ψ suppression by means of a model which may be considered as the quantum-mechanical analog of the formation time model, as described in [3, 15]. In this quantum-mechanical model, the $c-\bar{c}$ internal wave function fulfills a time-dependent Schrödinger equation. The effect of the surrounding medium is taken into account by means of a time-dependent real interaction potential. The same model had already been proposed in [4, 5, 7]. However, we improve the model on three points: (i) we use a "realistic" initial wave packet (see Sect. 3); (ii) we introduce an imaginary part accounting for the loss of probability due to the $D-\bar{D}$ coupling; (iii) we study the effect of a mixed phase in the plasma scenario.

The most important result of our investigation is the fact that the $p_\perp$-dependence of the suppression factor is very flat. This was already underlined in [4]. We have shown that this is really due to the quantum-mechanical description, even though the difference between the quantum-mechanical results and the semi-classical ones is less pronounced in the suppression factor (the quantity plotted in Fig. 13) than in the intrinsic survival probability of the J/ψ content in the plasma (see Fig. 5).

The realistic initial wave packet yields a stronger suppression in the plasma than for an initial J/ψ wave packet (see Fig. 2). As a result, the lifetimes involved (for the plasma and/or the mixed phase) should be rather small in order to reproduce the observed suppression ratio.

The coupling to the $D-\bar{D}$ channels plays a minor role (see Fig. 2), because, as already explained, the wave packet initially narrow, expands continuously and is absorbed when entering the absorption region. The J/ψ content, implying the wave packet at small r ($\lesssim 1$ fm) is not very much affected by the absorption happening at larger r. The situation is expectedly different for the ψ' or for other kinematical regions, as illustrated in [7].

The presence of a mixed phase produces of course additional , but limited, suppression. However, it is difficult to find information on its presence and on its lifetime from the comparison with experiment. The reason is that the data are not very sensitve to the plasma + mixed phase scenario. Since the flatness of the $p_\perp$-distribution results mainly from quantum mechanics, only the abso-

lute value of the suppression factor can serve as a constraint. Several unrealistic scenarios envisaged in Sect. 5 can be ruled out, but it is hard to discriminate between reasonable scenarios. The data seem to be compatible with a finite size plasma shrinking in a short time, possibly surrounded by a mixed phase also of short time. Let us notice however that in pure mixed phase scenarios, the data can accommodate a longer lifetime.

We want to discuss shortly some of the aspects of the model. The decoupling of the centre of mass motion from the relative motion is certainly an approximation, whose justification is yet to be done. Note that this problem has not been studied previously. The time-independence of the absorption potential is questionable also. One may wonder whether the coupling to the $D-\bar{D}$ channels changes inside matter. This question deserves to be investigated. On the other hand, the threshold of these channels are not expected to change drastically, because of the large mass of charmed quarks.

The Schrödinger model used here, although questionable, represents a definite improvement on the previous approaches. It seems to confirm the compatibility between the data and the plasma picture. The small lifetimes obtained in this work might indicate that the conditions for plasma formation are barely realized at the SPS energy. Of course, this does not rule out the alternative explanations. We plan to use this model to investigate the other charmonium states (χ, ψ', η_c) and, at higher energies, the bottonium states also.

References

1. T. Matsui, H. Satz: Phys. Lett. 178B (1986) 416
2. J.-P. Blaizot, J.Y. Ollitrault: Phys. Lett. 199B (1987) 499
3. F. Karsch, R. Petronzio: Phys. Lett. 212B (1988) 255
4. V. Cerny et al.: Z. Phys. C46 (1990) 481
5. J. Cleymans, R.L. Thews: Z. Phys. C45 (1990) 391
6. J. Cugnon, P.-B. Gossiaux: Europhys. Lett. 20 (1992) 31
7. J. Cugnon, P.-B. Gossiaux: Z. Phys. C58 (1993) 77
8. J.L. Richardson: Phys. Lett. 82B (1979) 272
9. F. Karsch, H.W. Wyld: Phys. Lett. B213 (1988) 505
10. S.P.K. Tavernier: Rep. Prog. Phys. 50 (1987) 1439
11. J. Badier et al.: Z. Phys. C20 (1983) 101
12. C. Kourkoumelis et al.: Phys. Lett. 81B (1979) 405
13. S.J. Brodsky, P. Hoyer, A.H. Mueller, W.K. Tang: Nucl. Phys. B369 (1992) 519
14. J. Cugnon, P.-B. Gossiaux: to be published
15. J.-P. Blaizot, J.Y. Ollitrault: Phys. Rev. D39 (1989) 232
16. C. Baglin et al.: Phys. Lett. 220B (1989) 471; 255B (1991) 459; 251B (1991) 465; 268B (1991) 453
17. C. Baglin et al.: Phys. Lett. 262B (1991) 362
18. C. Gerschel: in: Quark-gluon plasma signatures, p. 277, V. Bernard et al. (eds.). Gif-sur-Yvette: Edition Frontières 1991
19. D.M. Alde et al.: Phys. Rev. Lett. 66 (1991) 133
20. S. Gupta, H. Satz: Phys. Lett. 283B (1992) 439
21. H.W. Barz, B.L. Friman, J. Knoll, H. Schultz: Nucl. Phys. A484 (1988) 661
22. L.P. Csernai, J.I. Kapusta: preprint ISSN 0803-2696, Univ. of Bergen, 1992